Geotechnics for Sustainable Development - Geotec Hanoi 2013, Phung (edt). Construction Publisher. ISBN 978-604-82-0013-8

Creep behavior of marine clay under loading and unloading conditions

Hiroshi Matsuda
Yamaguchi University, Yamaguchi, Japan. E-mail: hmatsuda@yamaguchi-u.ac.jp
Tran Thi Phuong An
Yamaguchi University, Yamaguchi, Japan. E-mail: phuongan313@gmail.com
Hiroyuki Hara
Yamaguchi University, Yamaguchi, Japan. E-mail: hhara@yamaguchi-u.ac.jp

Keywords: pore water pressure, creep, swelling, pre-consolidation, elasto-visco-plastic model, cyclic loading

ABSTRACT: To develop an estimation method for the settlement-time relations of clay under cyclic loading condition, especially recognizing the effect of creep settlement on the swelling properties induced by unloading, reconstituted specimens of Tokyo bay clay were tested by using the Separate-Type Consolidometer. The results obtained in all stages of loading and unloading conditions were compared with the calculated ones using the elasto-visco-plastic model (EVP). In conclusion, the creep settlement including the creep swelling under the constant effective stress is affected by the intensity of unloading applied and under unloading condition, the creep settlement was observed.

1. INTRODUCTION

The major part of Tokyo Bay is composed of soft alluvial clays deposited after 10,000 years ago. The clays in the Bay are classified into high plastic clay ranging from 60% to 150% in water content (higher in the north and decreasing towards the south) (Hanzawa, 1979). In fact, Tokyo Bay includes about 249km^2 of reclaimed land area. Land reclamation has been carried out along the coast of Tokyo Bay since the Meiji period. The topography of the shoreline of Tokyo Bay differs greatly from that of the pre-modern period due to on-going land reclamation projects [source]. Therefore, the creep settlement of the above-mentioned clay occurred during reclamations cannot be controlled. So far, there are many researches on physically mechanical characteristic, consolidation behaviour under various loading conditions, and so on presented to public.

Today, there are some hypotheses on settlement time relationship of saturated marine clay when considering them including the scale effects such as hypothesis A, hypothesis B (Ladd) and hypothesis C (Aboshi). In this study, to clarify the effect of creep more in detail and also to estimate the settlement-time relations when cyclic loading is applied to the clay layer, the effect of creep on the consolidation during the unloading stage was investigated. This study is one of many experiments carried out to support the hypothesis C which assumes that creep occurs somewhere between hypothesis A and B.

2. EXPERIMENT, ANALYSIS METHODS AND REUSLTS

2.1 Experimental method

2.1.1 Reconstituted specimens

Based on the previous study, the fact that the time process of the settlement of marine clay coincides with Terzaghi's theory quite well, as the specimen was reconsolidated from slurry state (Aboshi, Matsuda, et al, 1981), Tokyo Bay clay samples used in this study are considered to be in the similar state. To prepare the reconstituted specimen, the samples were passed through a sieve of 420μm to exclude fragmented shells before being de-aired in the vacuum cell under the pressure of -98kPa. By using large scale consolidation cell (shown in Figure 2), reconstituted specimens were prepared. The consolidation stress of 4.2kPa, 9.8kPa, 19.6kPa, and 49kPa, respectively, were applied stepwise. Each stress was kept for 24 hours, but for the last one, consolidation duration was decided by the method of 3t. Then, samples were directly withdrawn by using thin wall tube with 7.4 cm in diameter.

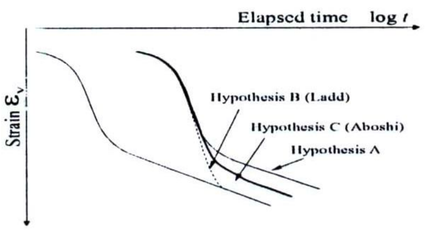

Figure 1. Hypotheses on settlement time relation in the scale effect

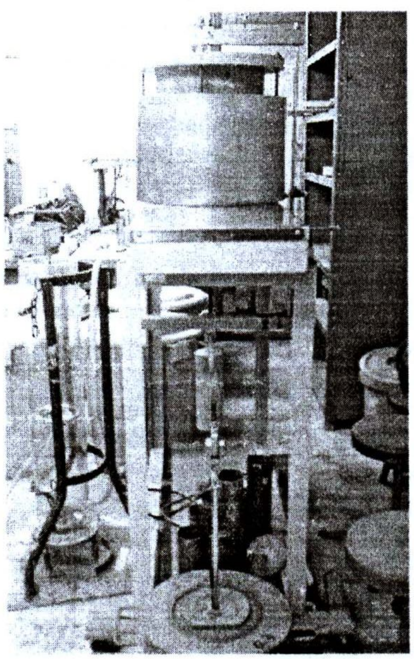

Figure 2. Vacuum cell and large scale consolidation cell to prepare the reconstituted specimen

Table 1. Physical characteristics of Tokyo Bay sample

ρ_s (g/cm^3)	2.78
w_L (%)	66.6
I_P	41.6
C_c	0.46
e_0	1.63
w_0 (%)	170.6

Physical characteristics of Tokyo Bay clay are shown in Table 1 and Figures 3 and 4.

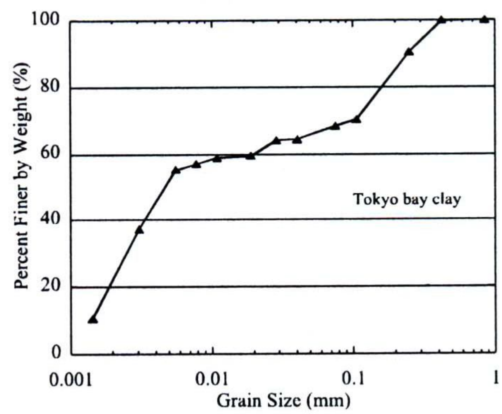

Figure 3. Grain size distribution curve of Tokyo Bay clay

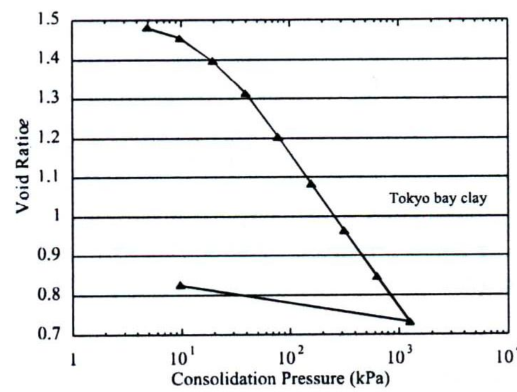

Figure 4. e-log P curve of Tokyo Bay Clay

2.1.2 Separate - Type consolidation test apparatus

In this study, the Separate-Type Consolidometer was used. This equipment consists of five oedometers of standard size, which are connected in series and loaded hydraulically under the predetermined pressure. It is proved to be very convenient to find the condition inside of a consolidating clay layer, because the strain and the pore water pressure at each divided specimen can be measured precisely, and because the consolidation pressure is applied to each sub-specimens directly, the effect of friction between the specimen and confining ring is minimized.

By using this apparatus, the specimen with thickness of 100mm and 60mm in diameter was divided into 5 sub-specimens of 20mm in thickness. Figure 5 and Figure 6 show the outline of the Separate-Type Consolidometer and a consolidation cell, respectively.

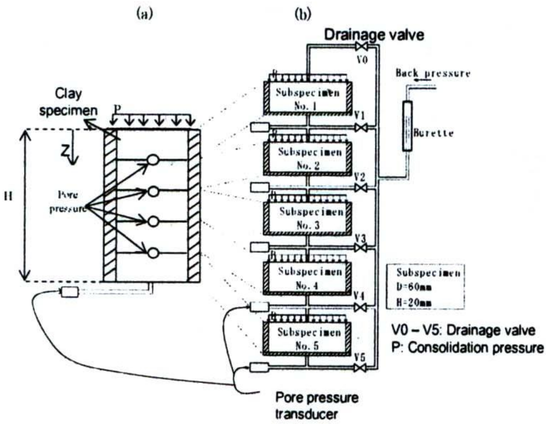

Figure 5. Outline of the Separate-type-consolido-meter

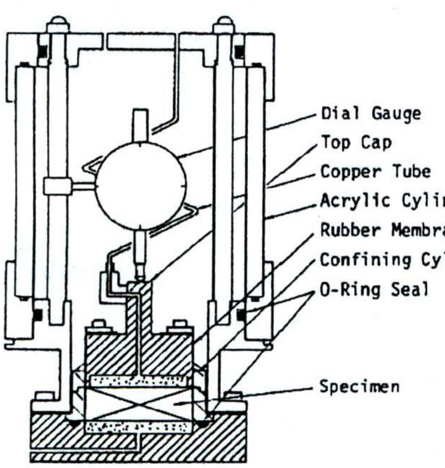

Figure 6. Outline of consolidation cell of the Separate-type-consolidometer

2.1.3 Loading condition

In this study, during the whole steps of consolidation test, the specimen was subjected to a back pressure of 98Kpa. The preparatory load of $\sigma_0/2$=39.2kPa and σ_0 = 78.4kPa, respectively, were applied. These kind of loading were kept until the end of primary consolidation (EOP).

After setting the valves to allow the drainage from the sub-specimens through the top surface of sub-specimen (No.1), each sub-specimen was applied to the main load of 156.8kPa and consolidated until the EOP. Then each sub-subpecimen was unloaded to the various loading levels as shown in Figure 7. In fact, the main load was kept until the EOP because the higher the degree of consolidation at the swelling stage, the smaller the residual settlement by the recompression in cyclic loading model (Aboshi and Matsuda, 1981). This study is a part of experimental series under cyclic loading condition, and the main objective of this study is to find out the effect of creep on swelling properties induced by unloading.

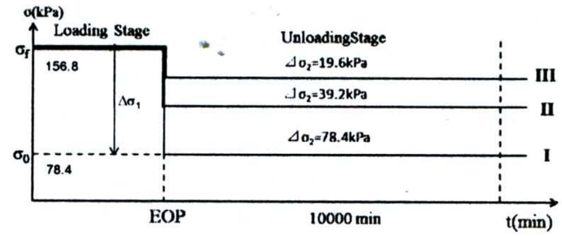

Figure 7. Loading level for the consolidation test

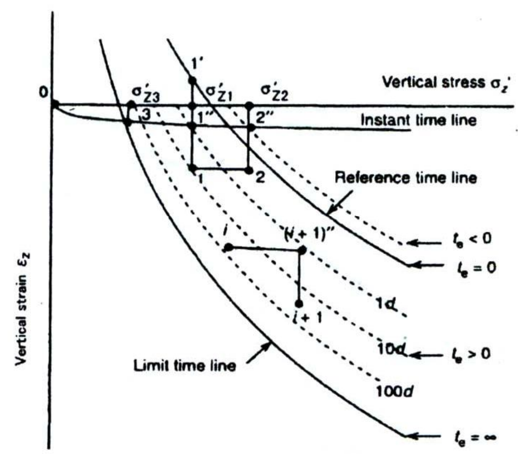

Figure 8. Illustration of instant time line, times lines, equivalent times, reference time line and limit time line (Yin & Graham, 1989b)

2.2 Analytical method

In this study, the experimental results were compared with calculated ones using the EVP (Yin and Graham 1996). This model belongs to the category of hypothesis B - creep occurs during the whole consolidation process (Suklie, 1957; Barden, 1965, 1969; Bjerrum, 1967).

Yin & Graham (1994) showed how elastic visco-plastic (EVP) modeling could be used to analyze the consolidation results by Berre and Iversen (1972). They found that the EVP model could simulate well the influence of straining rate, test duration, and relaxation on consolidation behavior. In this model, two parameters ψ and t_0 are used to describe time- dependent nonlinear creep in over consolidated, normally consolidated, and unload-reload ranges of stressing.

Yin & Graham (1996) developed the general elastic visco-plastic constitutive model for 1D straining (Yin & Graham 1989a, 1989b, 1994) which allows predicting some unanticipated pore water pressure responding in soft clays. The model developed the idea of "equivalent time" which relates to the duration of a current load increment to the time taken to creep from a "reference time line" obtained from normally consolidated results. The equivalent time t_e is the duration of straining at a constant effective stress σ'_z from a reference time line (t_e=0) to the current (σ'_z, ε_z, t_0) state, where ε_z is total vertical strain. The limit time in Figure 8 (Yin and Graham, 1989b) is defined as the time that has an equivalent time $t_e = \infty$, where a creep rate equal to zero. The behavior above the limit time line is time-dependent and elastic-visco-plastic. Below the limit time, it is time-independent.

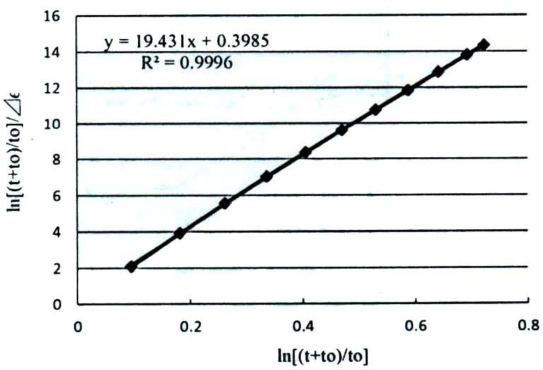

Figure 9. Curve fitting by a straight line for $\Delta\sigma$ = 78.4 kPa, to = 1000min

Yin and Graham (1999) showed a general equation for this model. If the equivalent time t_e is known, the strain at any state point (σ'_z, ε_z) is

$$\varepsilon_z = \varepsilon_z^{ep} + \varepsilon_z^{tp} = \varepsilon_{zo}^{ep} + \lambda/V\, ln(\sigma'_z/\sigma'_{zo}) + \psi/V\, ln[(t_o + t_e)/t_o] \quad (1)$$

where, t_e = the effective time shown by Yin & Graham (1996). κ/V, λ/V, ψ/V, σ', t_o and ε_o = six fitting parameters used in the model (Yin & Graham, 1994). In which, the variable V represents the specific volume of the clay. The parameter κ/V is similar to C_r, which defines unloading-reloading behavior. The parameter λ/V is similar to C_c, the compression index, which defines elastic-plastic behavior; σ'_{zo} has a somewhat similar role to the preconsolidation pressure p'_c, is related to initial void ratio e_o. The creep parameter ψ/V is similar to the coefficient of secondary consolidation $C_{\alpha e}$ (or $C_{\alpha\varepsilon}$) but is now independent of OCR, and t_o is similar to t_{EOP}, which shows the time at the EOP consolidation. However, the detailed definitions of these parameters used in the EVP model are not the same as those in the conventional approach.

Table 2. The EVP model parameters used for Tokyo Bay clay in this study

Parameters	Test No.	Value (unit)
V	I	2.31
	II	2.36
	III	2.33
κ		0.009
λ		0.17
ψ		0.01
k		6.03E-08 (cm/s)
t_0		1000 (min)
H_0	I	92.5 (mm)
	II	92.2 (mm)
	III	92.8 (mm)
σ_0		78.4 (kPa)
$\Delta\sigma_1$		78.4 (kPa)
$\Delta\sigma_2$	I	78.4 (kPa)
	II	39.2 (kPa)
	III	19.6 (kPa)

In this study, based on the approximate relationship between conventional consolidation parameters and the parameters in the 1D EVP model, κ, λ and ψ were calculated as shown below (Yin & Graham, 1999)

$$\kappa \approx \frac{C_r}{ln(10)},\quad \lambda \approx \frac{C_c}{ln(10)},\quad \psi \approx \frac{C_{\alpha e}}{ln(10)} \quad (2)$$

The parameter to were obtained by the new non-linear creep function (Yin.J.-H., 1999) that is simple to use

$$\Delta\varepsilon = \frac{\psi'_0 ln[(t+t_0)/t_0]}{1+(\psi'_0/\Delta\varepsilon_l)ln[(t+t_0)/t_0]} \quad (3)$$

where, $\Delta\varepsilon$ = creep strain; t = the creep time for a strain of $\Delta\varepsilon$; ψ'_o = ψ/V when t = 0; t_o = curve-fitting parameter related to choice of reference time line.

Equation (3) can be written as

$$\frac{ln[(t+t_0)/t_0]}{\Delta\varepsilon} = \frac{1}{\psi'_0} + \frac{1}{\Delta\varepsilon_l} ln\frac{t+t_0}{t_0} \quad (4)$$

If the total vertical strain is denoted by ε and the time by t_{total}, then the creep strain is $\Delta\varepsilon = \varepsilon - \varepsilon_{EOP}$ and the creep time is $t = t_{total} - t_{EOP}$.

Value of t_o is normally chosen in advance in the curve-fitting process. The measured data of creep strain $\Delta\varepsilon$ against creep time t are used to calculate the relationship of the normalized ratio $\ln[(t + t_o)/t_o]/\Delta\varepsilon$ to $\ln[(t + t_o)/t_o]$. However, Yin (1999) also showed that the parameter t_o could not be chosen arbitrarily. It was chosen in order that the R^2: the coefficient of determination was in the range $0 < R^2 < 1$. In this study, t_o is chosen as 1000 min, which can make the data points lying on a straight line (Figure 9). This, therefore, produces the best curve fitting based on equation (4).

Parameters used in EVP model for this study are shown in Table 2.

2.3 *Results*

2.3.1 *Temporal change of excess pore water pressure*

As mentioned above, by setting valve system sub-specimens were connected at the load of 156.8kPa. The excess pore water pressure was measured by a portable data logger.

Figure 10 shows a change of excess pore water pressure with elapsed time during the loading and unloading stages. The pore water pressure decreases gradually during the first loading stage and reaches the EOP, and immediately after the unloading, the negative pore water pressure increased and gradually recovered. Then the larger the unloading intensity, the greater the negative pore water pressure obtained.

The recovery process of negative pore water pressure is shown in detail in Figure 11. At the beginning of the swelling process, the values of negative pore water pressure is almost the same for z/H = 0.2 and for z/H = 1.0. This means that the distance from the drainage boundary does not affect the unloading-induced negative pore water pressure. In Figure 12, the relationships between $u/\Delta\sigma_u$ and time are shown, where $\Delta\sigma_u$ shows the unloading intensity. Comparing the results for different unloading intensities, the recovery of pore water pressure occurs more quickly at the lower unloading intensity. Similar tendencies in both the observed and calculated results are obtained in the whole consolidation process. However, the negative pore water pressure by using Yin's model are higher than that of observed ones.

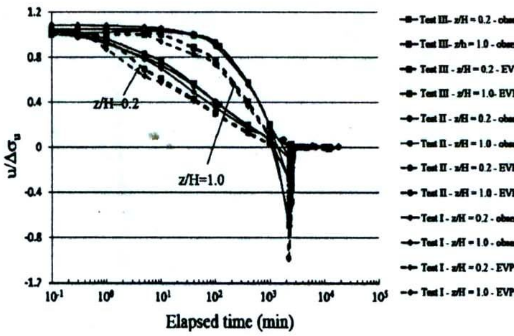

Figure 10. Change of pore water pressure during the consolidation process

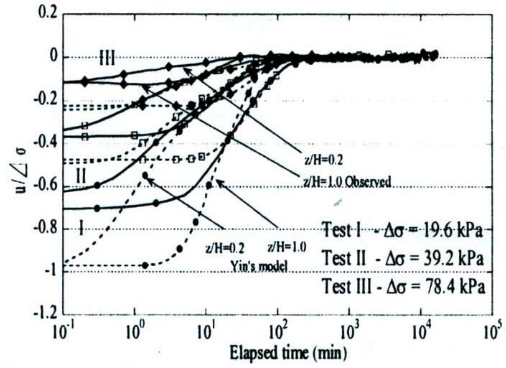

Figure 11. Change of pore water pressure during the swelling process ($\Delta\sigma$ = 78.4kPa : loading intensity)

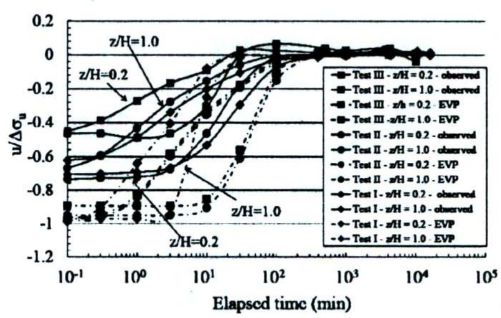

Figure 12. Change of pore water pressure during the swelling process ($\Delta\sigma_u$: unloading intensity)

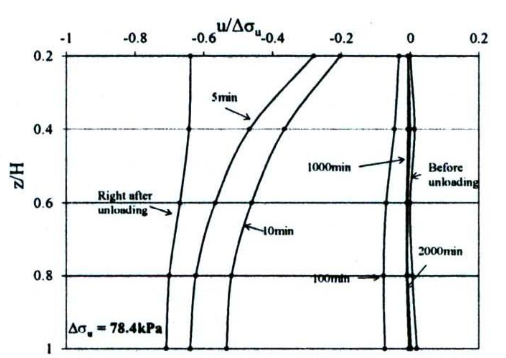

Figure 13. Change of pore water pressure with the depth in the case of $\Delta\sigma$ = 78.4kPa

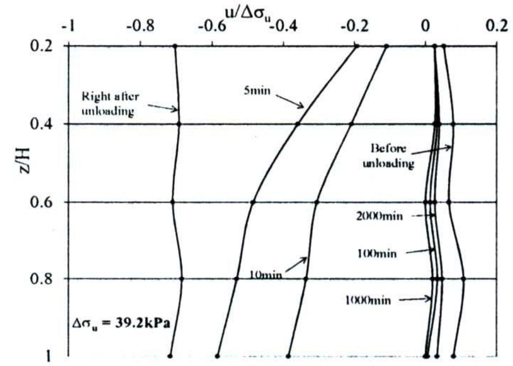

Figure 14. Change of pore water pressure with the depth in the case of $\Delta\sigma$ = 39.2kPa

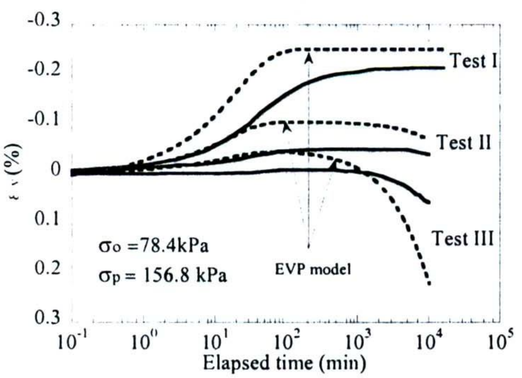

Figure 15. Changes of strain during unloading stage

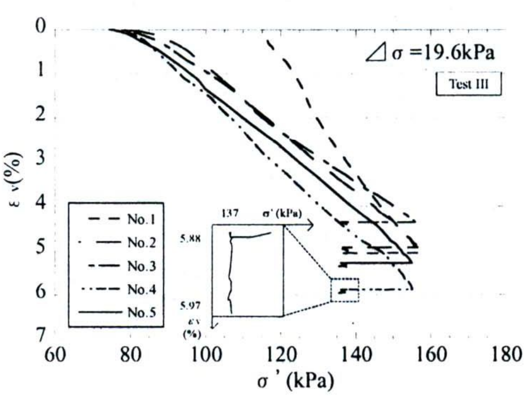

Figure 16. Relationships between effective stress and strain

The distribution of pore water pressure before and immediately after unloading for each layer shows a trend of parallel corresponding to unloading intensity. The greater the stress unloading, the greater the negative pore water pressure. The distributions of pore water pressure in three tests were observed at 5; 10; 100; 1000 and 2000 minute after unloading, which shows more clearly the movement in parallel irrespective of unloading intensity (Figure 13 and Figure 14). The distribution under different unloading intensities shows the same shape at any time points. For each loading, at the point of 5 min and 10 min, the distribution is quite different from the other points. At these times, the swelling of No.1 and No.2 occurred much more quickly than that of other sub-specimens because of their distances from the drainage surface. When the swelling of pore water pressure is gradually stable under a constant loading, the distribution lines become parallel in comparison with initial time points.

2.3.2 The change of strain with time during consolidation test

Figure 15 shows the change of strain ε_v with time during the unloading stage. The larger the unloading intensity, the larger the swelling occurs and the swelling is continued even after the pore water pressure reaches almost zero. This means that the swelling of specimen occurs under the constant effective stress. EVP model shows that the larger strain occurs compared with the observed one. In the case of test III ($\Delta\sigma_u$ =19.6 kPa), it is seen that the rate of swelling decreases and the settlement conversely starts to occur. Similar tendency is seen in the case of test II ($\Delta\sigma_u$ = 39.2 kPa) and in the calculated results.

Since it is easy to see the creep settlement in the case of Test III, the relationships between the strains and effective stress for each sub-specimen are shown in detail (Figure 16). No.1 shows the sub-specimen at the drainage boundary and No 5 as the undrainage boundary. During the loading stage, the settlement increases with the effective stress and after reaching about 157kPa, the effective stress decreases to 137kPa. Then it is seen that the settlement starts to occur. This means that the creep induced by the pre-loading is still remained even in the unloading.

3. CONCLUSIONS

To clarify the effect of creep on the settlement, especially during the unloading stage, saturated clay was subjected to the unloading after EOP by using the Separate-Type Consolidometer and the observed results were compared with EVP model. It is shown that the distance from the free drainage boundary does not affect the unloading-induced negative pore water pressure. Meanwhile, the creep settlement of specimens including the creep swelling under the constant effective stress is affected by the intensity of unloading applied, and in spite of the unloading condition, the creep settlement was observed and the similar results were obtained in EVP model.

4. REFERENCES

Aboshi, H. (1973). An experimental investigation on the similitude in the consolidation of a soft clay, including the secondary creep settlement, *Proc.8th ICSMFE*, Moscow, 4.3, pp 88.

Aboshi, H., H. Matsuda & M. Okuda (1981). Precomperssion by Separate- type consolidomater. *Pro. 10th ICSMFE (Stockholm)* pp. 577-580.

Aboshi, H., H. Matsuda (1983) A study on precompression technique by Separate- type consolidometer. *Jour. Geotech Eng. JSCE* No.340.pp. 139 – 144.

Aboshi, H., Yoshikuni, H. and Maruyama, S. (1970) "Constant loading rate consolidation test". *Soil and Foundations*, Vol.10, No.1, pp 43- 56.

Baek, J., Matsuda, H., Ishikura, R., Baek, W., Yamada, K (2012). Study on one- dimensional consolidation of saturated clay based on the relationship between effective stress relaxation and creep strain. *Jour. Geotech Eng. JSCE* Vol.68, No.2, pp 400-409.

Barden, L. (1965). Consolidation of clay with non-linear viscosity. *Geotechnique* 15, No.4, pp 345-362.

Berre, T. & Iversen, K. (1972). Oedometer tests with different specimen heights on a clay exhibiting large secondary compression. *Geotechnique* 22, No.1, pp 53-70.

Bjerrum, L. (1967). Engineering geology of normally consolidated marine clays as related to the settlements of buildings. *Geotechnique* 17, No.2, pp 83-119.

Garlanger, J.E. (1972). The consolidation of soils exhibiting creep under constant effective stress. *Geotechnique* 22, No.1, pp 71-78.

Hanzawa, H. (1979). Undrained strength characteristics of an alluvial marine clay in the Tokyo Bay. *Soils and Foundations* 19, No.4, pp 69-84.

Leroueil, S., Kabbaj, M., Tavenas F. and Bourchard, R. (1985). Stress- strain- strain rate relation for the compressibility of sensitive natural clays. *Geotechnique* 35, No 2, pp 159-180.

Mesri, G. (1973). Coefficient of secondary compression. *J. Soil Mech. Edn Engng Div., Proc. Am. Soc. Civ, Engrs* 99, SM1, pp 123-137.

Watabe, Y., Udaka, K., Kobayashi, M., Tabata, T., and Emura, T. (2008). Effect of friction and thickness on long-term consolidation behavior of Osaka bay clays. *Soil And Foundations*, Vol. 48, No.4, pp 547-561.

Yin, J. H. and Graham, J. (1996). Elastic visco-Plastic modeling of one-dimensional consolidation. *Geotechnique* 46, No. 3, pp 515-517.

Yin, J.-H, Graham, J. (1994). Equivalent times and one – dimensional elastic viscoplastic modeling of time – dependent stress – strain behavior of clays. *Can.Geotech*, J.31, pp 42-52.

Yin, J.-H, Graham, J. (1999). Elastic viscoplastic modeling of the time – dependent stress – strain behavious of soils. *Can.Geotech*, J.36, pp 736-745. [source] http://en.wikipedia.org/wiki/Tokyo_Bay>

Yin, J.-H, Graham, J., Clark, J I.Gao, L. (1994). Modeling unanticipated pore-water pressure in soft clays. *Can.Geotech*, J.31, pp 773-778.

Yin, J.-H. (1999). Non – linear creep of soils in oedometer tests. *Can.Geotech*, J.49, No. 5, pp 699-707.

Yin, J.-H. and Graham, J. (1989). Viscous-elastic-plastic modeling of one – dimensional time – dependent behavior of clays. *Can. Geotech*, J.26, pp 199-209.